Article

Modeling and Simulation of Heavy-Lift Tethered Multicopter Considering Mechanical Properties of Electric Power Cable

Hyeok-Min Kwon [ID] and Dong-Kyu Lee *

Department of Aeronautical and Mechanical Design Engineering, Korea National University of Transportation, 50 Daehak-ro, Chungju-si 27469, Korea; ghm8260@naver.com
* Correspondence: dklee@ut.ac.kr

Abstract: In case of a fire at a high-rise building which is densely populated, an extension ladder is used to rescue people who have yet to evacuate to a safe place away from the fire, whereas those who are stranded at a height that is unreachable with the ladder should be promptly saved with different rescue methods. In this case, an application of the tethered flight system capable of receiving power over a power cable from the ground to a multicopter may guarantee effective execution of the rescue plan at the scene where fire is raging without any restrictions of the flight time. This article identified restrictions that should be considered in the design of a multicopter capable of tethered flight aimed to rescue stranded people at an inaccessible location with an extension ladder at a fire-ravaged high-rise building and assessed its feasibility. A power cable capable of providing dozens of kilowatts of electricity should be installed to enable the implementation of the rescue mission using the tethered multicopter. A flexible multi-body dynamics modeling and simulation with viscoelastic characteristics and heavy weight of power cable were carried out to evaluate the effects of such cable of the tethered flight system on the dynamic characteristics of the multicopter. The results indicate that as for a heavy-lift tethered multicopter designed to be utilized for rescue operations, the properties of the power cable, such as weight, rigidity and length, have a major impact on the position and attitude control performance.

Keywords: multicopter; heavy lift; tethered flight; flexible multi-body dynamics

1. Introduction

In contrast with the past when unmanned air vehicles (UAVs) were originally used for military operations, such as reconnaissance or surveillance, they are now being proactively employed for civilian purposes. You can easily find in reality a variety of cases where they are put in use, ranging from drones for Amazon Prime Air delivery services in the US which are capable of carrying an item less than 2.26 kgf, through unmanned aerial vehicles from AeroVironment offering observation services and communication support at a fire scene and Google's SkyBender engaging in 5G wireless communication testing, to flying autonomous robots developed by Tevel Aerobotics Technologies to grow fruits without any wastes of human resources by selecting fruits of optimum quality based on their size and conditions [1–4]. eVTOL (electric Vertical Takeoff and Landing) vehicles, including multicopters as most representative, are at the center of the situations where unmanned aerial vehicles are being more widely used in the civil application. In particular, multicopters, which are capable of hovering, have been utilized in more diverse areas. Existing helicopters can also hover and have the advantage of being superior to multicopters in terms of payload capacity and endurance. However, they are mechanically complex because they require mechanisms such as a transmission system to transmit the rotational motion produced by turbine or piston engine to the rotor blades, and a swashplate for cyclic and collective control. Most multicopters do not need additional transmission system because each propeller is directly connected to the out-runner type BLDC motor. In addition, since

every propeller has pair to rotate at the same speed in opposite directions, gyroscopic precession caused by the spinning rotor can be neglected in many cases, and cyclic control is not required as it has symmetrical aerodynamic characteristics. The forces for attitude control are generated by changing the rotational speed of the motor. For those reasons, multicopters do not have to use a swashplate and can carry out control commands more frequently. It is also possible to guide a relatively safe landing even if one of their propellers fails since most of multicopters has more than four propellers. Based on these advantages, a research on space application of multicopter is also in progress. NASA Jet Propulsion Laboratory (JPL), in collaboration with AeroVironment Inc., NASA Ames Research Center and NASA Langley Research Center, has developed a vehicle capable of vertical take-off and landing on Mars [5,6] as shown in Figure 1, and the vehicle has succeeded in several flight tests on Mars. The Mars Helicopter, named Ingenuity, is an eVTOL vehicle equipped with a coaxial rotor which is composed of two propellers rotating in opposite directions. In order to reflect the difference in gravity between Earth and Mars during the flight test of the demonstration model of Ingenuity, an electrical tether was used to supply power from the ground while removing the battery [7,8]. The technological advancements of the electrical propulsion system, such as propellers, electric motors and batteries, have led to the recent development of large manned multicopters aimed to be integrated into the Urban Air Mobility (UAM) ecosystem [9–11].

(a)   **(b)**
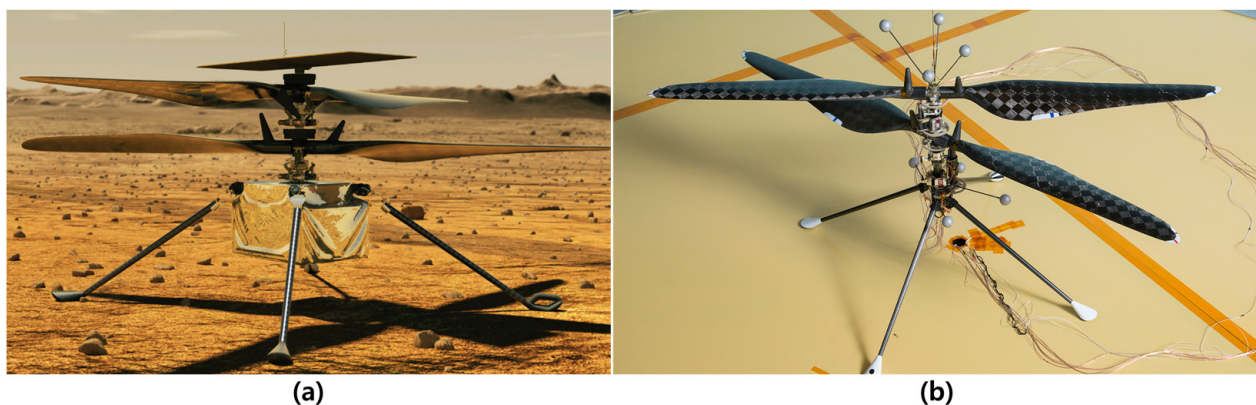
Figure 1. Example of space application of multicopter: (**a**) illustration of Mars Helicopter Ingenuity [6]; (**b**) demonstration model of Mars Helicopter powered through an electrical tether hanging below the vehicle during controlled-flight test [8].

Meanwhile, eVTOL sufficiently large enough to carry passengers is expected to be effective in rescue operations in case of a fire or disaster. In the process of industrial development, the urban concentration phenomenon, in which many people flock to the city, has resulted in high-rise buildings being built in large cities. As skyscrapers built mostly to accommodate residential places or office spaces are more densely populated than low-rise counterparts, they are likely to have relatively more severe damages when an accident or a fire breaks out, thus having various evacuation and preventive measures in place, including emergency staircase, emergency shelter or emergency lift. However, such evacuation and prevention measures may not cover all unexpected situations which leave some people stranded as they fail to promptly evacuate to a safe place, and generally a fire truck ladder directly accessible to the external wall of a high-rise building is used to rescue them. During the rescue operation of the people stranded at a high altitude using the aerial ladder, various restrictions are entailed [12]. A fire truck ladder consists of outriggers to hold the weight, a lift to carry people, an electric control system for the lift operation and a safety system to respond to an emergency. Table 1 shows the safe operational conditions of the constituents of the fire truck ladder. As the ideal climbing angle of the aerial ladder for safe operation ranges from 30 to 70 degrees, it can be used to carry out a rescue mission within an altitude lower than the actual length of the ladder. In addition, a clearance should be secured from the building where fire occurs depending on the climbing angle of the

ladder, which determines its reachable height. Generally, a clearance of approx. 13.7 m away from the external wall of the building is required to install an extension ladder as long as 50 m, whereas a 70-m-long ladder, used only in some cases to reach a high altitude, can have access to the height of up to approx. 64 m, which is about 24 story high given the average floor height (approx. 2.6~2.8 m) of an apartment building. In a situation where more skyscrapers with more than 30 stories are being built due to the above mentioned growth in the urban population, it becomes inevitable in some cases for some people to become trapped in a location higher than the height that the ladder can reach or impossible to secure a clearance to install the ladder. eVTOL vehicle capable of transporting passengers is deemed as an alternative solution to promptly rescue people.

Table 1. Safe operational conditions for elevated ladder of fire truck.

Components	Operational Constraints
Loading vehicle	Road slope $< 5°$ Ground rigidity should be ensured
Outrigger	Maximum allowable load: 80 T Deployment radius: 5.2 m Deployment angle: $-7°\sim70°$
Lift	Working speed: 1 m/s Ladder deployment angle: $30°\sim-70°$ Ladder deployment length: 23~53.2 m

Regular eVTOL vehicles are not capable of executing a long-duration mission due to limited battery capacity, but there were cases where a tethered flight system was developed to overcome such limitation of flight time. UCON Systems developed T-Rotor for military operations, and Israel Aerospace Industries (IAI) came up with Hover Mast in a joint partnership with Sky Sapience. There are several products capable of tethered flight, such as Elistair's safe-T and Power Line of Network Time Protocole, which replace the existing multicopters' power system [13–15] which are shown in Figure 2. However, as these tethered flight systems are used to provide electricity to and communicate with multicopters of small size designed mostly for observation and communication relay, the presence of power cable does not greatly affect the dynamic characteristics of multicopters.

Figure 2. Tethered multicopters and tethered flight system for multicopters: T-Rotor [13], Hover Mast [14], Power Line [15].

Weight and flexural rigidity of the power cable greatly changes depending on the operating voltage and current. As tethered multicopters for rescue purposes should be able to perform hovering flight with at least one passenger on board, there should be a heavy-duty power cable installed to ensure stable power supply from the ground, which generates a relatively large effect on flight dynamics brought by changes in the weight and flexural rigidity of the cable. In order to analyze the flight dynamic characteristics of a tethered multicopter, dynamics for each of the multicopter and the electric power cable should be modeled. Giernacki et al. [16] obtained information such as geometric

dimensions, masses and moment of inertial, which are major parameters of the equation of motion, from the technical documentation provided by the multicopter manufacturer. Ivler et al. [17] built a multicopter flight dynamics model close to reality by performing system identification using actual flight test data. In relation to the dynamic characteristics of the tethered system, various studies have been carried out especially for space applications. Aslanov et al. [18] conducted a study to identify the dynamic characteristics based on mathematical modeling of the space tethered system, which collectively refers to applications such as space escalator, space elevator, lifting and descent of a payload into an orbit and placing a spacecraft into orbit. Misra et al. [19] studied the transverse and longitudinal vibration of sub-satellite tethered to the space shuttle. Based on the modeling of the tether elevator system installed on both sides of the space station, Lorenzini et al. [20] investigated the dynamics of the space elevator to maintain the center of mass of the entire system within the space station by controlling the length change of a tether while the elevator is operated on the other tether. Williams et al. examined the influence of thermal induced flexibility change of tether on tethered aerocapture missions [21]. They constructed two temperature-dependent dynamics models of the tether based on Lagrange's equation and Kane's equation, respectively. Through numerical simulations, it was confirmed that the longitudinal stiffness of the tether has a significant effect on the maneuver of the entire system. There have been several studies on helicopters or multicopters with slung load [22–24], of which configurations are similar to tethered multicopters, but most studies were conducted on applications where the effects of mass and flexural rigidity of cables could be neglected.

This study analyzed restrictions integrated in the design of tethered multicopters for rescue mission, which require a heavy and thick power cable, to identify the requirements of the tethered flight system and the power cable. Based on the mechanical properties of the power cable obtained from bending tests, a flexible multi-body dynamics modeling was conducted on tethered multicopter with a power cable. Later, a simulation for position and attitude control was carried out, based on a model where the power cable of different lengths depending on the flight altitude was integrated, to observe change in flight dynamics of the multicopter.

2. Design of Heavy-Lift Tethered Multicopter

2.1. Mission Profile

Multicopters can be used to perform lifesaving missions in areas inaccessible to firefighting ladders or where there are restrictions on the deployment of elevated ladders. However, the battery-equipped multicopter has a relatively short endurance due to limited battery capacity, so it cannot reliably perform rescue missions for a long time. The size of multicopter should be suitable for lifesaving operations without causing an accident and interfering with the performance of other workers' missions after arriving at the site regardless of the method of transport to the fire or disaster site. In addition, it is required to guarantee good flight performance in various conditions such as ascending flight for approach, hovering while on board and descending flight for landing during rescue missions. Figure 3 shows the operational process of a tethered multicopter for rescue purposes. Once an emergency is reported, fire trucks and multicopters are immediately dispatched to the emergency site. After arriving at the fire site, a safety space of a certain size necessary for multicopter take-off and landing must be secured. Once the safety space is secured, the conditions and location of stranded people should be identified in detail. When the detailed information is obtained, the heavy-lift tethered multicopter should start its flight for rescue mission. It has to hold not only its position to hover around the contact point, but also its attitude angles even when there exists weight shift while rescued person is boarding. After the multicopter safely lands on the truck and unloading the rescued person, it continues the rescue operation repeatedly until there are no people left in the building. After the execution of such a mission, the power supply system and the entire multicopter as well as its equipment should be checked, and in case repairs are required,

they should be carried out in line with the proper procedures with maintenance being conducted on a regular basis [25,26].
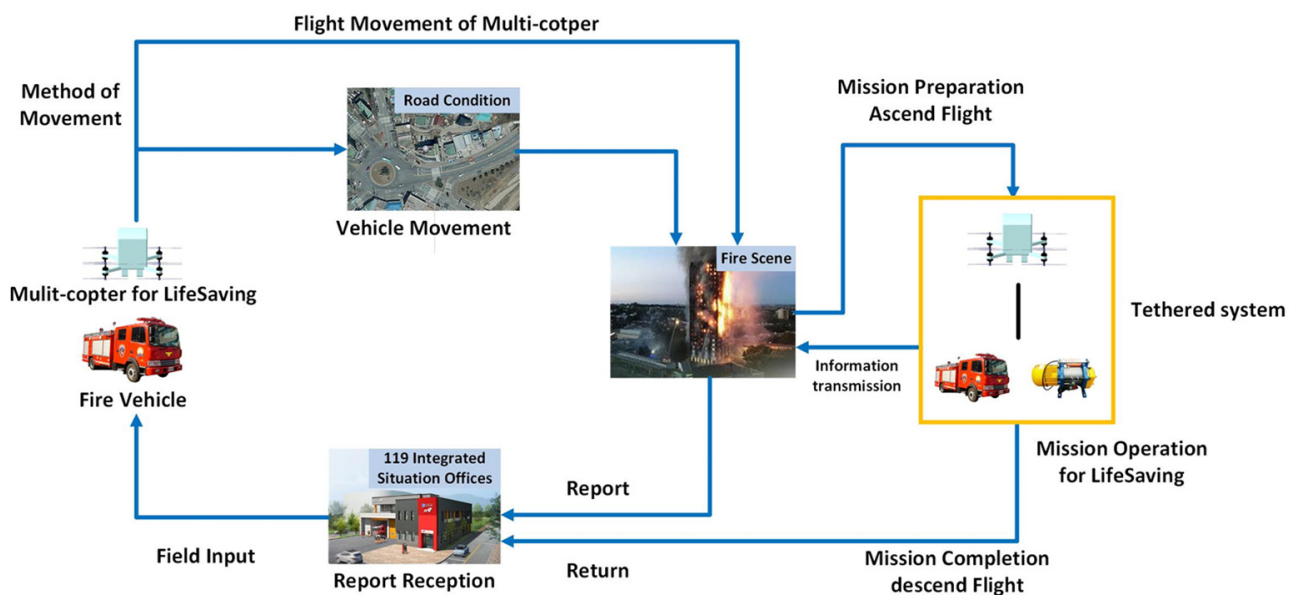

Figure 3. Mission profile of heavy-lift tethered multicopter for lifesaving mission.

2.2. Analysis on Design Constraints

2.2.1. Size Constraints

A tethered multicopter is required to rapidly move to a site where fire or disaster occurs to execute a rescue operation. There are two ways for them to move to the scene: first, they fly to the site directly and connect to on-site infrastructure, such as a fire hydrant or streetlamp, to be supplied electric power from ground for tethered flight. Second, they are loaded onto an existing automotive vehicle, retrofitted for this purpose, to be transported to the site. As multicopters have autonomous flight capability, they are able to move quickly to the scene unaffected by the traffic conditions without any assistance of an additional loading vehicle. However, this requires the establishment of infrastructure, as a precondition, that includes a power supply system near high-rise building, a traffic control system and spatial information of downtown areas required for flights of large eVTOL in the urban area. The second way of moving the tethered multicopter to the scene which involves a loading vehicle has its limitation as it is affected by traffic conditions and may result in belated arrival, but there is an upside as well in that the loading vehicle can carry the power supply system and equipment for the mission as well as additional devices, guaranteeing stable execution of the operation. As a result, it is concluded that transporting the multicopter tethered to the loading vehicle is more effective than direct flight to a fire or disaster site, and if it is designed in a size enough to be loaded onto a fire truck with water pump dispatched to a fire scene, it will be easily transported on the road. Table 2 shows a list of overall length, width and height of each size of generally used fire trucks with water pump. Considering the expected size of a multicopter that can lift at least one person and the applicability in cramped urban areas, the frame width and length of the multicopter are decided as 1800 mm and 2400 mm, respectively. This size of multicopter allows the small fire pump car can be retrofitted to load the tethered multicopter.

2.2.2. Weight Constraints

As multicopters for rescue purposes should be able to take off and land vertically with passengers on board, they should share similar capabilities with eVTOL vehicles that are being developed to be integrated into UAM ecosystem. eVTOL vehicles to be incorporated into the UAM ecosystem is classified as the following three categories: vectored thrust,

lift-cruise and multicopter. In case of the vectored thrust and lift-cruise types, which are capable of vertical take-off/landing and long-range cruise flight, they need an additional fixed wing structure as well as additional mechanisms for propulsion system. As for rescue missions at a fire site which require repeated vertical take-offs and landings while receiving electricity from the power cable within a limited range, without cruise flight, the multicopter type is most suitable. Table 3 shows the specifications of UAM vehicles of multicopter type that are currently being developed. Among them, Ehang 184, a vehicle whose performance was verified in numerous flight tests and which is of relatively simple structure, was chosen as a reference to analyze the weight-related constraints of tethered multicopters for rescue missions.

Table 2. Size of various types of fire pump car.

Type	Length (mm)	Width (mm)	Height (mm)
Large	8500	2500	3400
Medium	8000	2500	3200
Small	6800	1900	2800
Light	5200	1200	2800

Table 3. Specifications of multicopter type heavy-lift eVTOL.

Manufacturer	Ehang	Airbus	Volocopter
Model	Ehang 184	City Airbus	2X
Size (m)	4 × 3.9 × 1.4	8 × 8	3.2 × 9.15 × 2.15
MTOW (kgf)	360	2200	450
Payload (kgf)	100	250	150

As the tethered multicopters receive power from the ground via power cable, battery can be removed from the vehicle and the tethered flight system can be loaded as much as the weight of the battery. Ehang 184 is known to use a lithium-based secondary battery, which widely powers various electric mobilities because it has relatively high energy and power density, long life expectancy and excellent temperature stability. The capacity of the battery loaded in Ehang 184 is known to be 14.4 kWh, and when the weight energy density of a small lithium-ion battery of about 117 wh/kgf is applied, the weight of the battery can be estimated to be about 123 kgf [27–29]. Accordingly, the total weight of the mooring flight system including the weight of the power cable that changes in proportion to the flight altitude should not exceed 123 kgf at the maximum flight altitude.

2.2.3. Initial Design of Tethered Flight System

For the flight of a tethered multicopter for rescue purposes, electrical power should be supplied to the electric propulsion system via power cable, and the size of the current flowing through the power cable varies depending on the size of the supplied voltage. Assuming that the power consumption during hovering flight is about 57.8 kW, the same amount to that of Ehang 184, a current of about 480 A must be transmitted through the power cable from the ground with DC power of 120 V. The weight per unit length of the power cable, in this case, is estimated to be about 1.5 kgf/m to meet IEC 60,227 standard. While a couple of power cables are required for DC powe supply, the maximum length of the cable is about 40 m if the weight of the existing battery is all converted into the weight of the power cable. This concludes that it is impossible to perform the rescue mission at a higher altitude compared to the existing fire truck ladder.

Since the weight of the power cables per unit length depends on the current that runs through them, the supplied voltage should be increased to deliver same amount of electric power. For many power transmission applications, three-phase four-wire AC scheme is adopted to minimize electric current and increase transmission efficiency. The weight of the power cable per unit length can also be reduced with this scheme. Meanwhile, as they should be flame-retardant because they are used at a fire site, HF-CO, TFR-CV and TFR-8 cables, which are widely used for high supply voltage and temperature applications, can be used for this purpose. The weights per unit length of HF-CO, TFR-CV and TFR-8 cables were measured as 0.78 kgf/m, 0.79 kgf/m and 0.83 kgf/m, respectively, and Figure 4 indicates the maximum ceiling of the tethered multicopter with those power cables depending on the weight of an AC/DC converter to be loaded onto the airframe. 600 V was considered as the supply voltage for the three-phase and four-wire system. When the weight of the AC/DC converter of the tethered flight system is 50 kgf [30], the ceiling altitude according to the application of HF-CO, TFR-CV and TFR-CV is calculated as 94 m, 93 m and 88 m, respectively.
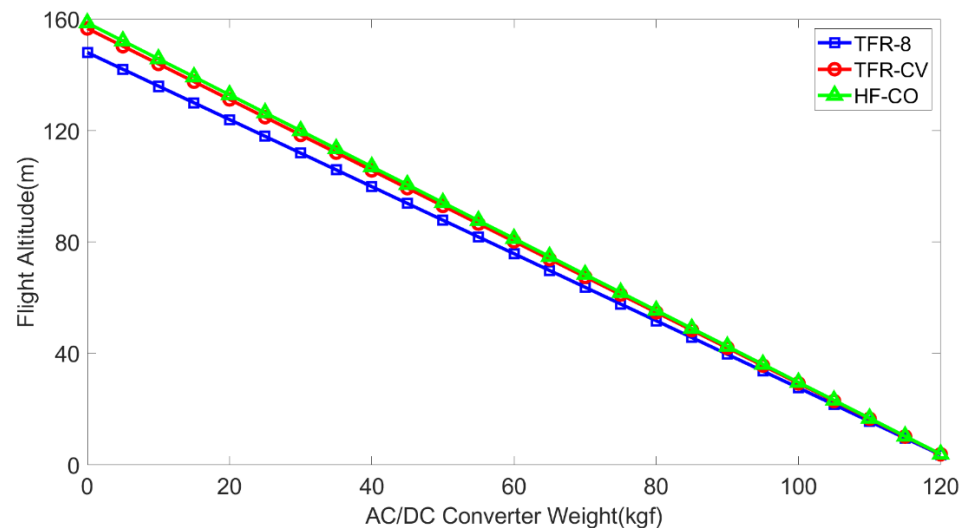
Figure 4. Maximum flight altitude of the tethered multicopter for various types of power cable according to the weight of AD/DC converter.

The layout of the tethered multicopter for rescue purposes in consideration of the above restrictions relevant to the size and weight is shown in Figure 5. At the bottom of the loading space of the small fire pump car, there should be a power supply system with a capacity of 100 kW as well as a winch that adjusts the length of the power cables depending on the flight altitude, and the airframe should include the AC/DC converter that properly distributes electricity from the three-phase four-wire AC power source to each BLDC motor, and flight control systems.
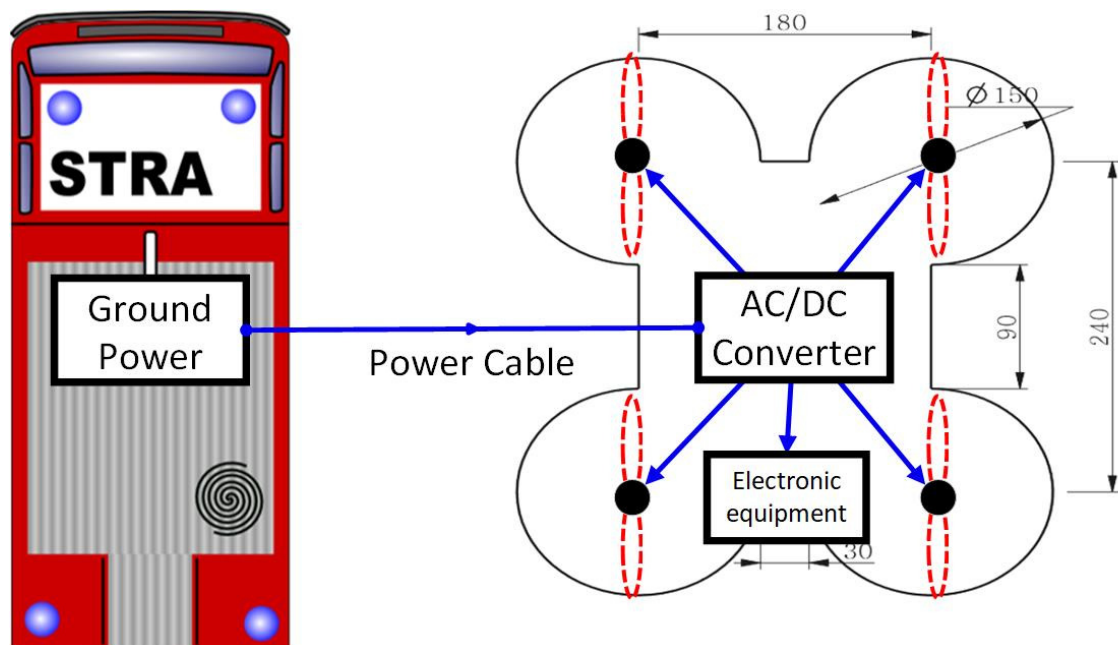
Figure 5. Layout of heavy-lift tethered multicopter for lifesaving Mission.

3. Flexible Multi-Body Dynamics Simulation of Heavy-Lift Tethered Multicopter

3.1. Mechanical Properties of Power Cable

The weight and flexural rigidity of the power cable, one of the main components of the tethered flight system, can have a significant effect on the dynamic characteristics of the heavy-lift tethered multicopter. It is required to identify the weight and flexural rigidity of the power cables for dynamics modeling of the tethered multicopter, and especially, it is extremely difficult to theoretically evaluate the flexural rigidity of the cables made of complex materials, including conductor, insulator, binder tape and sheath. To estimate the flexural rigidity of the cables in an experiment, a bending test on cantilever structures built with power cables were carried out as shown in Figure 6.
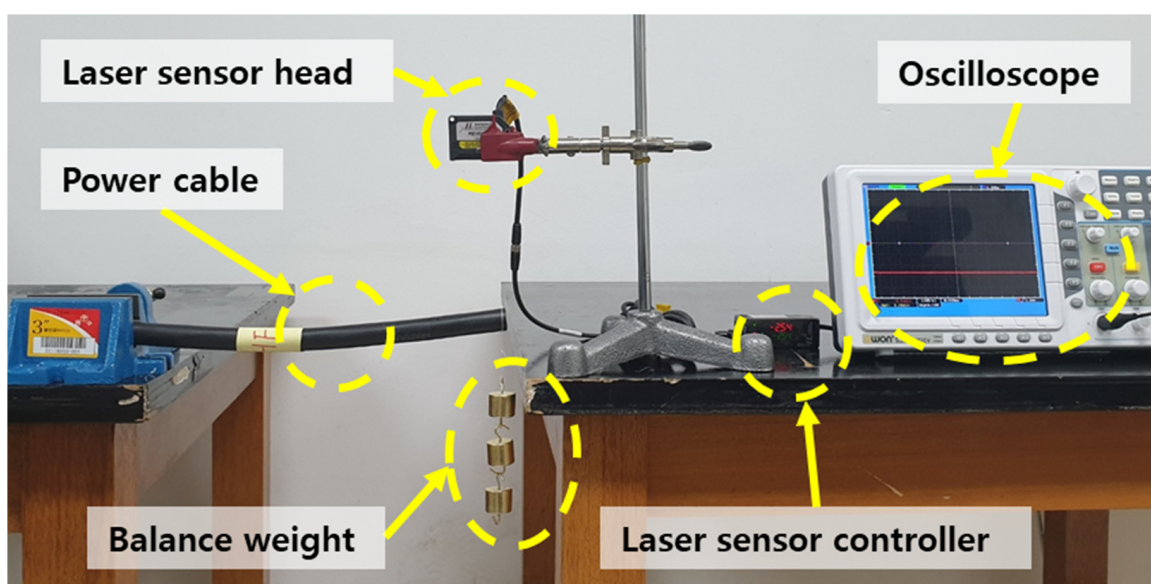

Figure 6. Experimental setup for measurement of flexural rigidity of power cable.

To calculate the equivalent flexural rigidity of the cables based on the test results, the cables were assumed to be made of isotropic material, and the correlation between the applied load and the free end displacement as shown in Equation (1) was used.

$$\delta = \frac{FL^3}{3(EI)_{eq}} \tag{1}$$

δ refers to the free end displacement, F is the applied load on the free end, L is the length of the power cable and $(EI)_{eq}$ means the equivalent flexural rigidity of the power cables. In order to reduce errors due to clearance, storage conditions and cutting methods while preparing the specimen, bending tests were carried out repeatedly with multiple specimens.

3.1.1. Static Bending Test

In order to proceed the bending tests, four specimens for each type of power wire of HF-CO, TFR-CV and TFR-8 were prepared, and the detailed specifications of each specimen are shown in Table 4. After clamping a power cable specimen as a cantilever, a laser sensor was located to measure the free end displacement. Balance weights were used to apply load at the free end of the specimen. The free end displacement for each applied load was measured after it converged to a certain value.

Table 4. Dimensions of power cable specimen.

| Cable Type	Length (mm)	Diameter (mm)	Weight Per Unit Length (kgf/m)
HF-CO	400	17	0.78
TFR-CV	400	17	0.79
TFR-8	400	20	0.83

Figures 7–9 show the relationship between the free end displacement and the applied load, and the calculated equivalent flexural rigidity for each type of power cable. The coefficients of determination of each bending test with HF-CO, TFR-CV and TFR-8 cables were calculated as 0.998, 0.996 and 0.996, respectively. It shows that structural characteristics of power cables are linear. Table 5 summarizes the equivalent flexural rigidity of each power cable calculated from the experimental results. Even though the dimensions and electrical characteristics of the power cables are similar, the equivalent flexural rigidity may vary depending on the cable type. It can be expected that the dynamic characteristics of the heavy-lift tethered multicopter, based on the above results, are significantly affected by the types of power cable applied for the electric power transmission.

Table 5. Equivalent flexural rigidity for various types of electric power cable.
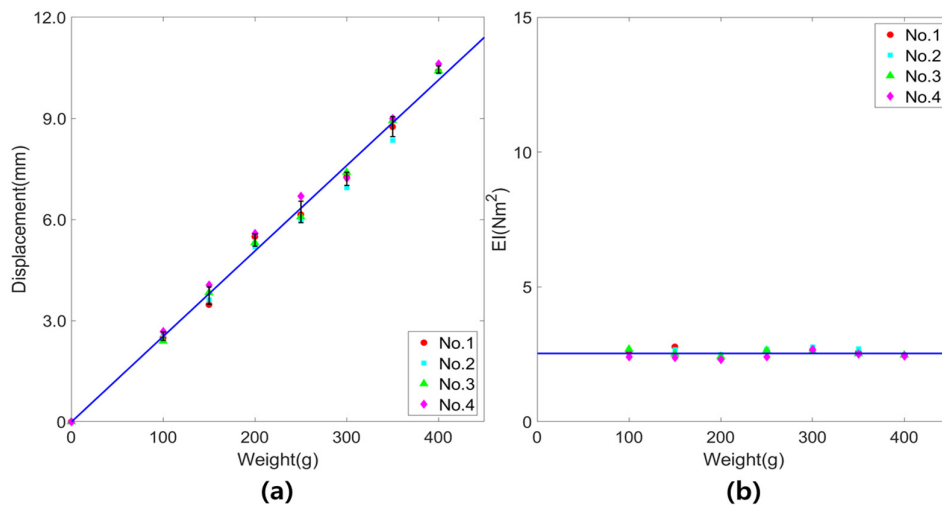
Cable Type	Equivalent Flexural Rigidity (Nm^2)	Standard Deviation (Nm^2)
HF-CO	9.74	0.48
TFR-CV	5.66	0.42
TFR-8	2.53	0.13
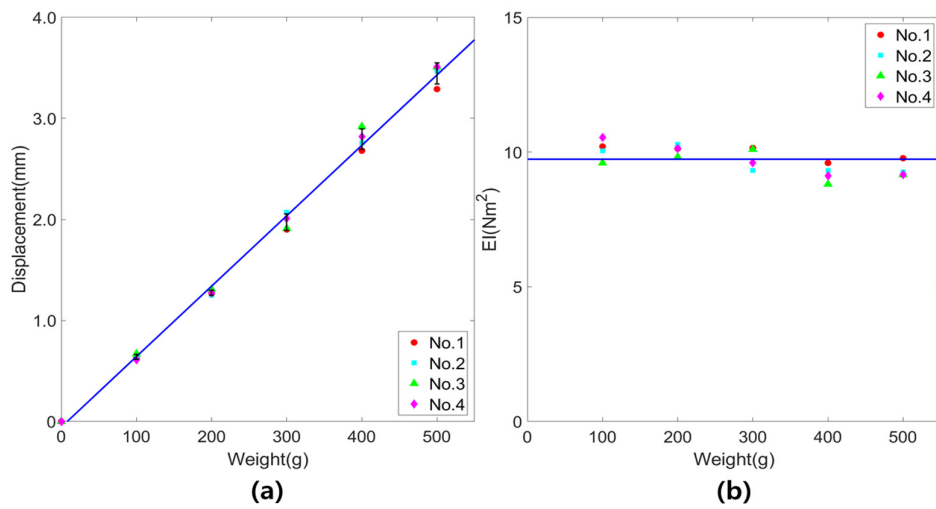
Figure 7. Static bending test results for HF-CO: (**a**) Free end displacement versus applied load (coefficient of determination: 0.998); (**b**) Equivalent flexural rigidity.
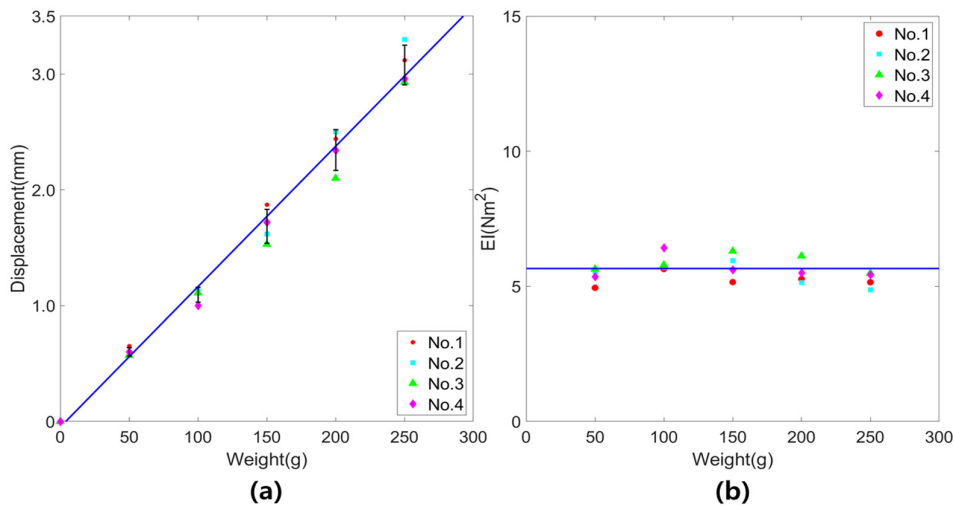
Figure 8. Static bending test results for TFR-8: (**a**) Free end displacement versus applied load (coefficient of determination: 0.996); (**b**) Equivalent flexural rigidity.

Figure 9. Static bending test results for TFR-CV: (**a**) Free end displacement versus applied load (coefficient of determination: 0.996); (**b**) Equivalent flexural rigidity.

3.1.2. Consideration of Viscoelasticity

As mentioned above, it takes several minutes for the level of displacement to converge to a certain value after a balance weight is applied on the free end of the power cable. It may be attributed to creep, which leads to an assumption that power cables are made of viscoelastic materials. Once a load is applied on a viscoelastic material, an elasticity-induced displacement is immediately observed and subsequently a displacement triggered by viscosity starts to be slowly created. To generate a model of such viscoelastic material, one of the following models is usually utilized: Maxwell model, Kelvin-Voigt model, Zener model and Burgers model [31,32]. Maxwell model, which consists of linear spring and linear viscous dashpot, is adopted in this study to estimate the flexural rigidity of the power cables in a more accurate manner and the formula used is shown below in Equation (2)

$$\frac{d\varepsilon}{dt} = \frac{1}{E}\frac{d\sigma}{dt} + \frac{\sigma}{\eta} \tag{2}$$

where ε means strain, η refers to viscosity, which could change depending on various factors, such as temperatures and the conditions of the power cable specimen.

Viscosity can be expressed as a damping coefficient of a power cable by expressing Equation (2), which is a relational expression between stress and strain, as a relation between force and displacement. In order to consider the viscoelasticity of the power cable, the change in the displacement according to the application of the free end load was measured in time domain. Figure 10 shows the change in the displacement of a TFR-CV specimen; balance weight of 100 gf was applied and removed at about 5 min, and 15 min, respectively, after the measurement was started. δ_k is the displacement made by the linear spring, whereas δ_η means the displacement triggered by the linear viscous dashpot. The equivalent flexural rigidities obtained through the previous static bending tests were the result of adding the displacement by the linear spring and the linear viscous dashpot. Therefore, if the equivalent flexural rigidity of the power cable is more accurately calculated by considering only the displacement caused by the linear spring excluding the linear viscous dashpot, a larger value will be obtained than the result measured through the static bending test. According to the maxwell model, the section in which displacement due to the viscous dashpot is observed can be assumed as a first-order linear function as shown in Figure 11.
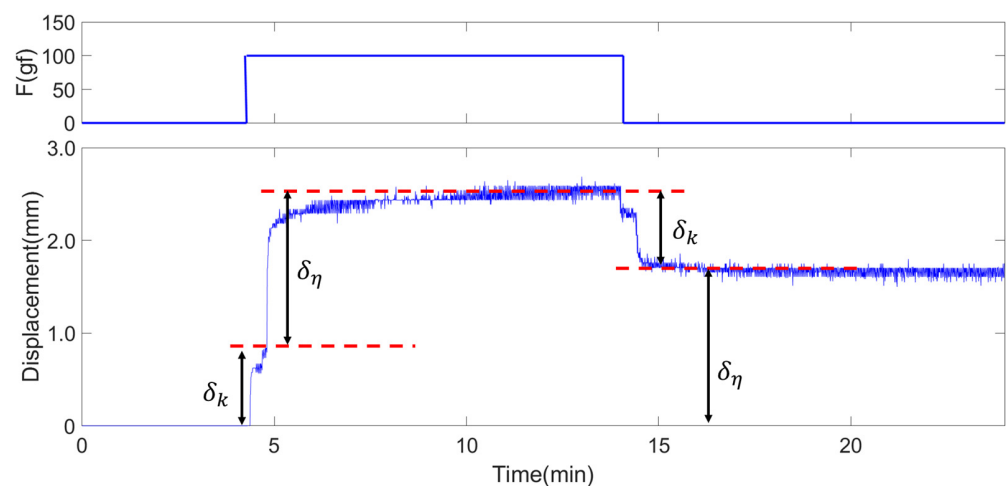
Figure 10. Free end displacement changes in time domain due to viscoelasticity.

Table 6 summarizes the results of measuring the maximum displacement and permanent displacement for each TFR-CV specimen. By applying the linear Maxwell model to the results, the damping coefficient and the equivalent flexural rigidity of TFR-CV were calculated as 6.5×10^5 Ns/m and 7.14 Nm², respectively. Considering the creep effect, the

updated equivalent flexural rigidity is about 2.5 times larger than the previous result. It can be seen that the flexural rigidity of the heavy-duty power cable measured by a static bending test is accompanied by a large error, and it is necessary to perform a bending test considering viscoelasticity in order to obtain more sophisticated structural model of the power cable.
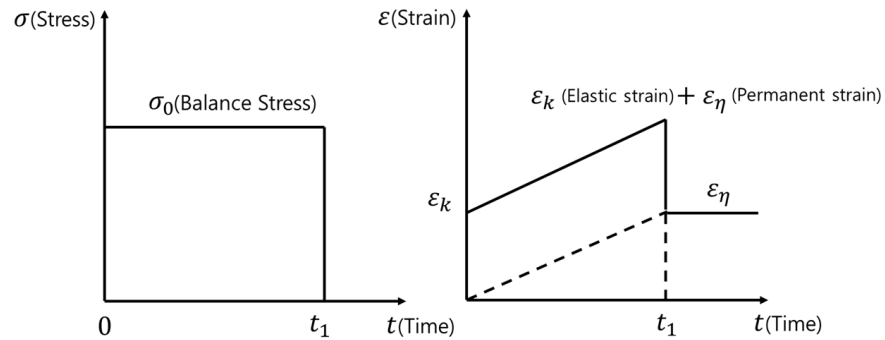

Figure 11. Maxwell model in creep and recovery.

Table 6. Displacement due to linear spring and linear viscous dashpot effect of TFR-CV specimen.

Measured Displacements	No. 1	No. 2	No. 3	No. 4
Maximum displacement ($\delta_k + \delta_\eta$) [mm]	2.53	2.67	2.72	2.51
Permanent displacement (δ_η) [mm]	1.57	1.88	1.77	1.62

3.2. Position and Attitude Control Simulation of Tethered Multicopter

3.2.1. Flexible Multi-Body Dynamics Modeling

Using the mechanical properties of the power cable that consist of the tethered flight system, a multi body dynamics model can be constructed. The motion of the power cable can be analyzed with the Euler-Bernoulli beam theory if the bending displacement of the power cable is small. In case of large bending displacement is expected, however, pseudo-rigid-body method, elliptic integral solution, domain decomposition method, chain algorithm or circle-arc method are used for mathematical modeling [33,34]. The properties of the power cables obtained in the previous test were used to create DEM (Discrete Element Model), composed of multiple links and springs, by dividing the entire power cables into *n* parts as shown in Figure 12.
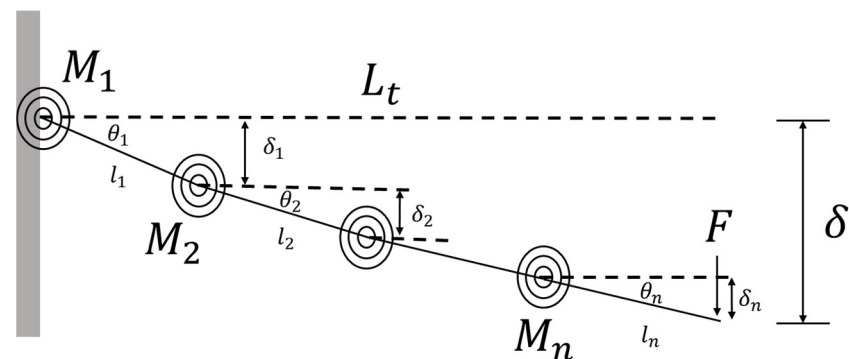

Figure 12. Flexible multi-body modeling method for the power cable structure.

Assuming that the angular change of the torsion spring exists within the linear range, the moment of the torsion spring M_i can be expressed as Equation (3) while satisfy the following condition, $i \leq n$.

$$M_i = k_i(\theta_i - \theta_{i-1}) \tag{3}$$

As the cantilever bending test was conducted in static, the linkage-spring model also should be in a static state. Equation (3) can be adopted to calculate the moment taken for each linkage as shown in Equation (4).

$$Fl_i = M_i - M_{i+1} \tag{4}$$

By assuming that k_n is an equivalent spring constant of the cantilever divided into n equal parts, the free end displacement of the linkage-spring model can be estimated as Equation (5).

$$\delta = \delta_1 + \delta_2 + \cdots + \delta_n = \frac{FL_t^2}{k_n}\left(\frac{1}{n^2}\right)\left(\frac{n(n+1)(2n+1)}{6}\right) \tag{5}$$

Since the free end displacement of the cantilever obtained from Equation (1) matches with Equation (5), the equivalent spring constant of the linkage-spring model can be calculated as shown in Equation (6).

$$k_n = \frac{(n+1)(2n+1)}{2n}\frac{(EI)_{eq}}{L_t} \tag{6}$$

Using the damping coefficient derived from Equation (2) and the equivalent spring constant derived from Equation (6), structural model of the power cable was obtained. In addition, the power cable model is combined with the flight dynamics model of a multicopter to construct the flexible multi-body dynamics model of a heavy-lift tethered multicopter as shown in Figure 13a. To analyze the altitude control and roll attitude control command-following performance of the tethered multicopter for various conditions, a flexible multi-body dynamics simulation was performed using MATLAB Simulink and RecurDyn which is commercial CAE software focused on multibody dynamics. Since it was difficult to obtain various parameters required to perform dynamic simulation of heavy-lift multicopter, the dynamic modeling of the multicopter part was relatively simplified compared to the electric power cable part. For mass and moment of inertia arranged in Table 7, values roughly estimated from the results of 3D modeling using the published specifications of Ehang 184 were used, and the effect of viscous friction or drag due to air flows was assumed to be negligible while performing simulations in conditions close to hovering. The maximum thrust that each of the eight propellers installed in the multicopter could produce was calculated by dividing the thrust equal to twice the maximum take-off weight by 8, the number of propellers. The power cable was divided into 10 linkages, and each couple of linkages were connected by a revolute joint to limit its motion within a plane. A torsional spring was added on each revolute joint and its equivalent torsional spring constant was calculated by substituting the flexural rigidity of the power cable, which was obtained from the previous test, into Equation (6).

3.2.2. Position and Attitude Control Simulation

An environment as shown in Figure 13b was created to simulate position and attitude control of the tethered multicopter with power cables consisting of multiple links and springs. Feedback control simulation was performed on roll, pitch, yaw attitude and altitude of the multicopter by importing the flexible multi-body dynamics model to MATLAB simulink while independent PID control scheme was employed for each degree of freedom. Two flight altitude conditions of 5 m and 90 m were selected to observe the change of dynamic characteristics according to the flight altitude of the tethered multicopter. The simulations were conducted with two torsional spring constants of TFR-CV, $k_{nominal}$ and $k_{Maxwell}$, in order to confirm that the correct flexural rigidity of the power cable should be used when the dynamics model of the heavy-lift tethered multicopter is constructed.

The flight altitude control of the multicopter is achieved through the overall increase/decrease of the thrust generated by each rotor, so it is possible to minimize the

effect of flexural rigidity of the power cable due to the change in the attitude angle of the multicopter during altitude control simulation. As shown in Figure 14, there were no significant difference in command following performances according to the torsional spring constant of the power cable while the overall performance in the low altitude condition is superior to that in the high-altitude condition. This is thought to be due to the fact that the weight of the entire vehicle was increased by the power cable suspended under the multicopter in case of high-altitude conditions.
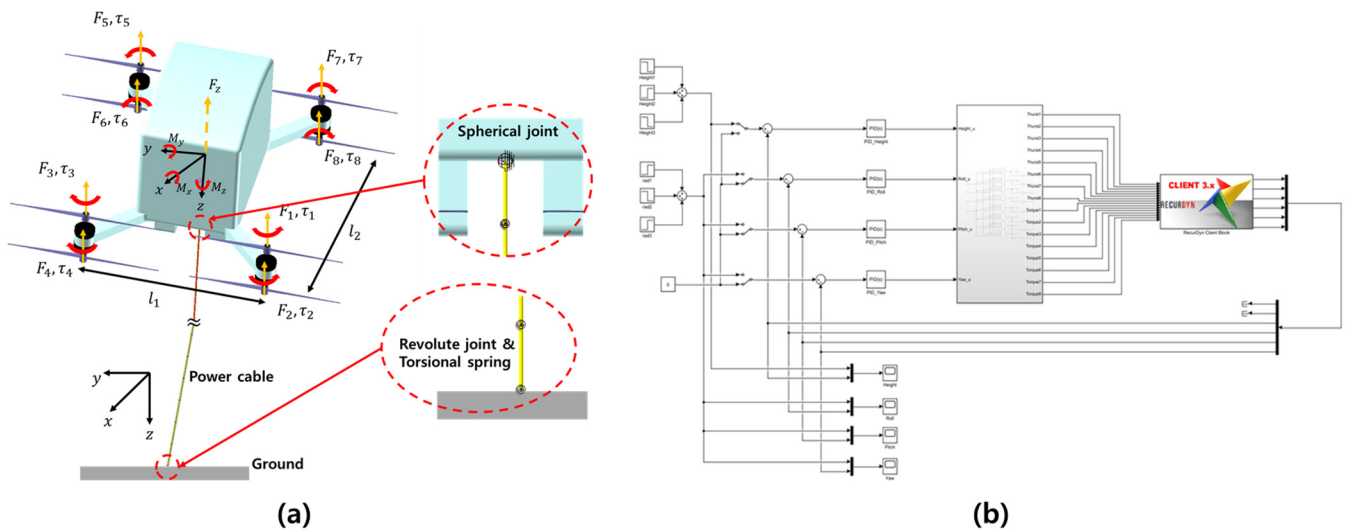
Figure 13. Position and attitude control simulation of the heavy-lift tethered multicopter: (**a**) Flexible multi-body dynamics model; (**b**) Block diagram for height and attitude control simulation.

Table 7. Mass and moment of inertia of the heavy-lift multicopter without electric power cable.

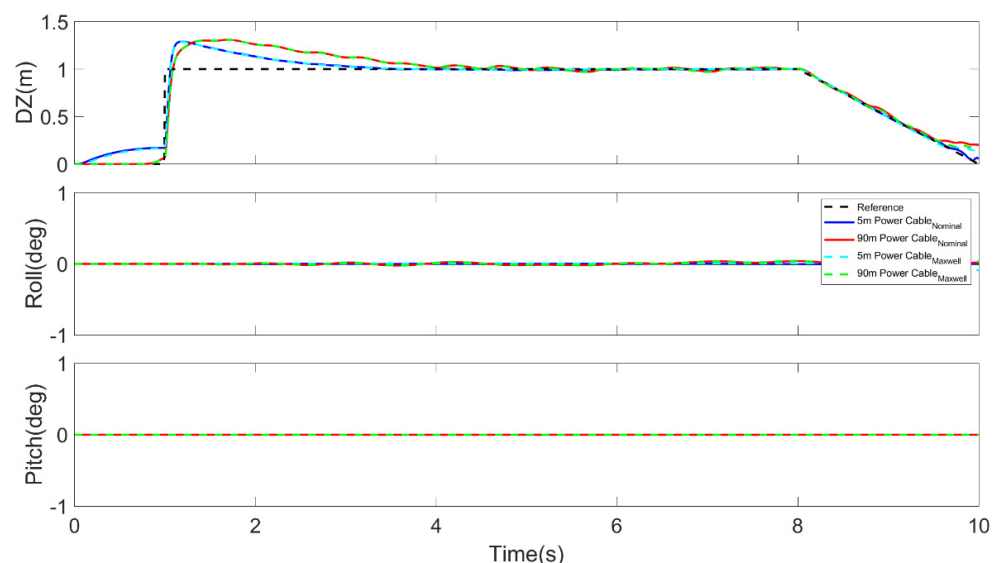| Mass (kg)	Moment of Inertia (kg mm^2)	
m = 137	$I_{xx} = 3.30 \times 10^9$ $I_{yy} = 4.88 \times 10^9$ $I_{zz} = 4.39 \times 10^9$	$I_{xy} = 7.39 \times 10^3$ $I_{yz} = -6.65 \times 10^2$ $I_{zx} = -5.86 \times 10^2$

Figure 14. Altitude, roll and pitch attitude of the tethered multicopter during altitude control simulation for various torsional stiffnesses and altitude conditions.

The result of comparing the roll attitude control performance is shown in Figure 15. It is confirmed that the roll attitude control performance is slightly worse at high altitude conditions, which is thought to be due to the difference in the weight of the power cable. However, in case of the horizontal direction, a larger motion was observed in the high-altitude condition than in the low altitude condition even though it was caused by the same roll attitude maneuver. This difference in horizontal movement according to the flight altitude is attributed to the length of power cable because the cable ties the multicopter to the ground when it is fully stretched as shown in Figure 16.
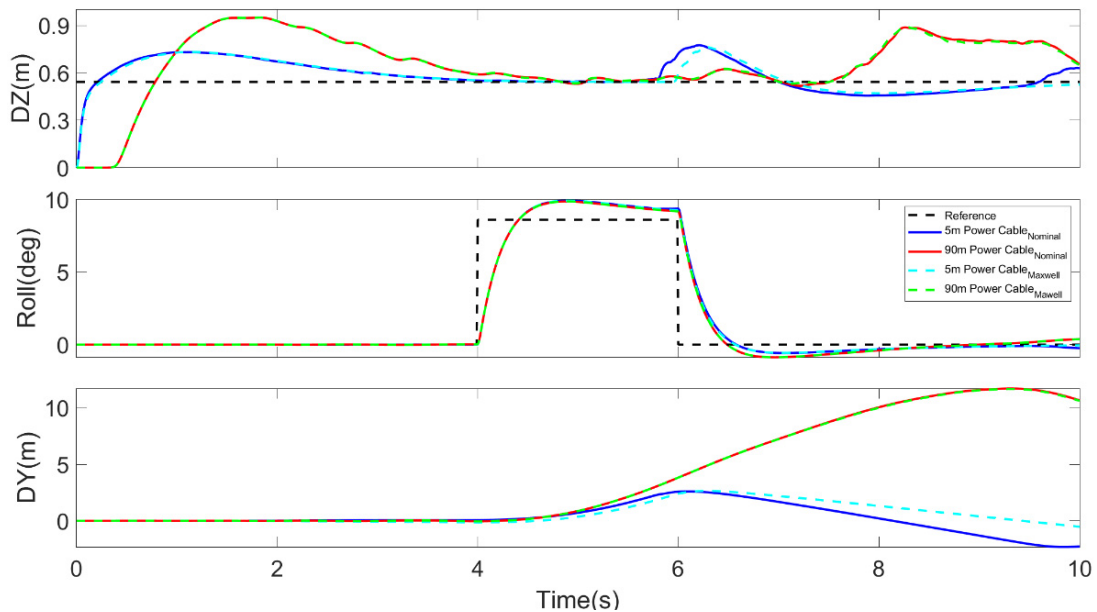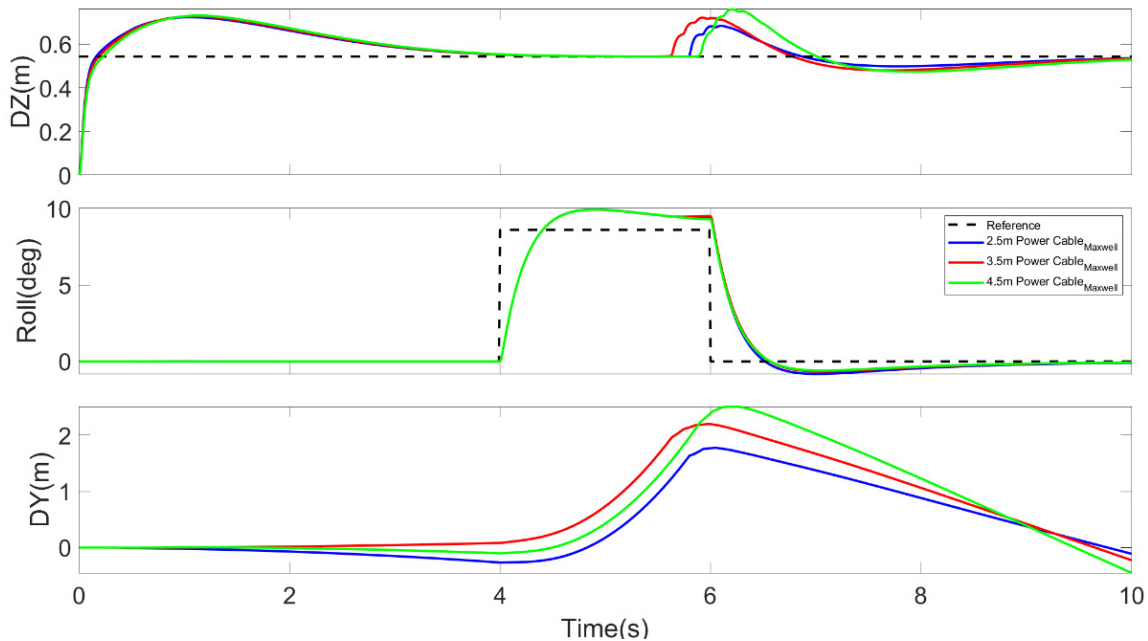

Figure 15. Altitude, roll attitude and horizontal position of the tethered multicopter during roll maneuver control simulation for various torsional stiffnesses and altitude conditions.
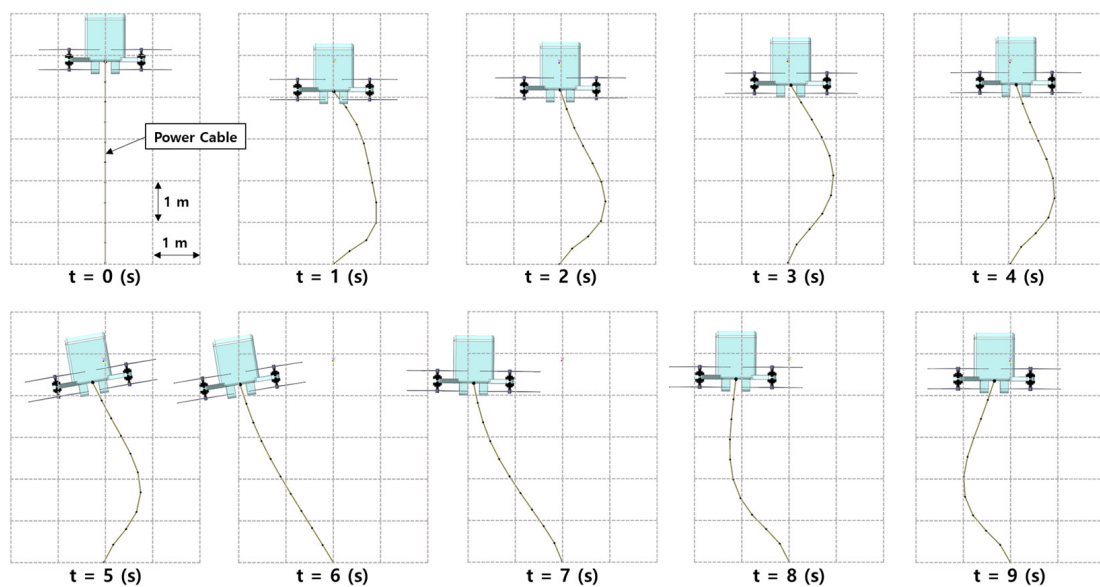
Figure 16. Front view of the tethered multicopter captured every second during roll maneuver control simulation at 5 m altitude.

Meanwhile, significant effect of the flexural rigidity of the power cable on the horizontal motion is observed at low altitude condition in contrast with at high altitude condition.

For more detailed analysis, simulations with the same roll command were conducted at flight altitudes of 2.5 m, 3.5 m and 4.5 m. As shown in Figure 17, there are relevant differences in horizontal motion with the same roll attitude maneuver despite the short altitude change. It can be concluded again that the flexural rigidity of heavy-duty power cable should be considered to obtain high control performance during take-off and landing at low altitudes.

Figure 17. Altitude, roll attitude and horizontal position of the tethered multicopter during roll maneuver control simulation for various altitude conditions.

4. Conclusions

When people are isolated at the scene of a fire in a high-rise building in an urban area, rescue is usually carried out by means of a fire truck with elevated ladder. However, in situations where it is impossible to secure the required space for operation of the elevated ladder or when people are isolated at a higher position than the elevated ladder can reach, other effective countermeasures are required for lifesaving and heavy-lift multicopters which can vertically take-off and landing with people on board could be one of the alternatives. Typical multicopters are not suitable for long-term missions due to limited battery capacity, but if a tethered flight system that transmits electric power from ground through power cable is applied, lifesaving missions can be performed with the multicopter at a high-rise building fire site regardless of endurance. In this study, a feasibility study was performed on whether it is possible to deploy tethered multicopters for a rescue mission at urban fire sites. The size and weight constraints were derived based on the mission profile of the heavy-lift tethered multicopter, and the initial design of the tethered flight system was conducted to meet the requirements. Since it is possible for the tethered multicopter to remove the battery, it can load tethered flight system as heavy as the weight of the existing battery. The heavy-duty power cable occupies most of the weight of the tethered flight system, and three-phase four-wire AC system with high supply voltage should be applied to minimize the weight of the power cable. Given the above conditions, it is estimated that the tethered multicopter can climb up to more than 90 m if the electric power is supplied with the voltage of 600 V. The power cables that should transmit high power have high flexural rigidity and heavy weight per unit length. If one of those cables is attached under a multicopter, it can significantly affect position and attitude control performances of the vehicle. Flexible multi-body dynamics simulations were conducted to observe the change

in dynamic behavior according to the flight altitude, and the equivalent flexural rigidity of the power cable made of various complex materials was experimentally measured considering viscoelastic effect. The obtained flexural rigidity was used for structural modeling of the cable. According to the simulation results, the weight effect of the power cable was significant at high altitude condition while the flexural rigidity affected the vertical and horizontal motion a lot at low altitude condition. In particular, the low altitude condition is closely related with take-off and landing of the multicopter, and high accuracy position control performance is required for safe operation. In order to improve the position and attitude control performance of the heavy-lift tethered multicopter for lifesaving mission, gain scheduling or adaptive control scheme that can take into account the weight change for various altitude and flexural rigidity effect of the power cable at low altitude should be applied for its flight control system, and the performances of these control algorithms can be comparatively evaluated through feedback control simulations using the flight dynamics model obtained previously. Furthermore, the methodology used in this study is expected to be utilized to analyze the dynamic characteristics of space tethered systems and design control systems of them.

References

1. Alieksieiev, V.; Markovych, B. Implementation of UAV for environment monitoring of a Smart City with an airspace regulation by AIXM-format data streaming. *Industry 4.0* **2020**, *5*, 90–93.
2. Ramesh, P.S.; Jeyan, J.M.L. Comparative analysis of the impact of operating parameters on military and civil applications of mini unmanned aerial vehicle (UAV). *Proc. AIP Conf.* **2020**, *2311*, 030034.
3. Woźniak, W.; Jessa, M. Selection of Solar Powered Unmanned Aerial Vehicles for a Long Range Data Acquisition Chain. *Sensors* **2021**, *21*, 2772. [CrossRef] [PubMed]
4. Bogue, R. Fruit picking robots: Has their time come? *Ind. Rob.* **2020**, *47*, 141–145. [CrossRef]
5. Koning, W.J.; Johnson, W.; Grip, H.F. Improved Mars helicopter aerodynamic rotor model for comprehensive analyses. *AIAA J.* **2019**, *57*, 3969–3979. [CrossRef]
6. Illustration of Mars Helicopter. Available online: https://www.nasa.gov/aeroresearch/nasa-aeronautics-experts-help-prepare-ingenuity-to-fly-on-mars (accessed on 24 June 2021).
7. Grip, H.F.; Johnson, W.; Malpica, C.; Scharf, D.P.; Mandić, M.; Young, L.; Allan, B.; Mettler, B.; Martin, M.S.; Lam, J. Modeling and Identification of Hover Flight Dynamics for NASA's Mars Helicopter. *J. Guid. Control Dyn.* **2020**, *43*, 179–194. [CrossRef]
8. Mars Helicopter Prototype. Available online: https://mars.nasa.gov/resources/22372/mars-helicopter-prototype/ (accessed on 24 June 2021).
9. Hascaryo, R.W.; Merret, J.M. Configuration-Independent Initial Sizing Method for UAM/eVTOL Vehicles. In Proceedings of the AIAA AVIATION Forum 2020, Dalas, TX, USA, 17–19 June 2020; p. 2630.
10. Bacchini, A.; Cestino, E. Electric VTOL configurations comparison. *Aerospace* **2019**, *6*, 26. [CrossRef]
11. Busan, R.C.; Murphy, P.C.; Hatke, D.B.; Simmons, B.M. Wind Tunnel Testing Techniques for a Tandem Tilt-Wing, Distributed Electric Propulsion VTOL Aircraft. In Proceedings of the AIAA SciTech 2021 Forum, Nashville, TN, USA, 11–15 January 2021; p. 1189.
12. Beak, S.C. A Study of Fire-truck Design for the Possible Suppression and Respond of Initial Fire. Master's Thesis, Hongik University, Seoul, Korea, 2018.
13. UCON System. Available online: http://www.uconsystem.com/eng/products/military/trotor.asp (accessed on 15 June 2021).

14. Skysapience. Available online: https://skysapience.com/drone/hovermast-150-c/ (accessed on 24 June 2021).
15. Powerline. Available online: https://www.ntpdrone.com/product/ (accessed on 15 June 2021).
16. Giernacki, W.; Gośliński, J.; Goślińska, J.; Espinoza-Fraire, T.; Rao, J. Mathematical Modeling of the Coaxial Quadrotor Dynamics for Its Attitude and Altitude Control. *Energies* **2021**, *14*, 1232. [CrossRef]
17. Ivler, C.; Niemiec, R.; Gandhi, F.; Sanders, F.C. Multirotor Electric Aerial Vehicle Model Validation with Flight Data: Physics-Based and System Identification Models. In Proceedings of the VFS 75th Annual Forum, Fairfax, VA, USA, 13–16 May 2019; pp. 1–26.
18. Aslanov, V.S.; Ledkov, A.S. *Dynamics of Tethered Satellite Systems*; Woodhead Publishing Ltd.: Cambridge, UK, 2012.
19. Misra, A.K.; Xu, D.M.; Modi, V.J. On vibrations of orbiting tethers. *Acta Astronaut.* **1986**, *13*, 587–597. [CrossRef]
20. Lorenzini, E.C.; Cosmo, M.; Vetrella, S.; Moccia, A. Dynamics and control of the tether elevator/crawler system. *J. Guid. Control Dyn.* **1989**, *12*, 404–411. [CrossRef]
21. Williams, P.; Blanksby, C.; Yeo, S. Heating and modeling effects in tethered aerocapture missions. *J. Guid. Control Dyn.* **2003**, *26*, 643–654. [CrossRef]
22. Buler, W.; Sibilski, K.; Winczura, Z.; Zyluk, A. Nonlinear dynamics of helicopter with slung load analysis by continuation methods. In Proceedings of the 39th Aerospace Sciences Meeting and Exhibit, Reno, NV, USA, 8–11 January 2001; p. 110.
23. Notter, S.; Heckmann, A.; Mcfadyen, A.; Gonzalez, F. Modelling, simulation and flight test of a model predictive controlled multirotor with heavy slung load. *IFAC PapersOnLine* **2016**, *49*, 182–187. [CrossRef]
24. De Angelis, E.L. Swing angle estimation for multicopter slung load applications. *Aerosp. Sci. Technol.* **2019**, *89*, 264–274. [CrossRef]
25. Youn, G.H. Sersive Design for using the Drones in the Early Stages fires of Dense Residential Area. *J. Korean Contents Soc.* **2019**, *19*, 111–121.
26. Kim, K.T.; Park, M.S.; Park, S.W.; Park, S.H. The Concept of Operations of the Multicopter UAVs for Disater and Public Safety-Based on Mission Scenarios. *Curr. Ind. Technol. Trends Aerosp.* **2017**, *15*, 84–96.
27. Khofiyah, N.A.; Sutopo, W.; Nugroho, B.D.A. Technical Feasibility Battery Lithium to Support Unmanned Aerial Vehicle (UAV). In Proceedings of the International Conference on Industrial Engineering and Operations Management, Bangkok, Thailand, 5–7 March 2019; pp. 3591–3601.
28. Ogumi, Z.; Sutopo, W.; Nugroho, B.D.A. *Lithium Secondary Batteries*; A-JIN Publishing Co., Ltd.: Seoul, Korea, 2019.
29. Critique of Battery Powered Flying Car. Available online: https://moller.com/brochures/Critique-of-Battery-Powered-Flying-Cars.pdf (accessed on 24 June 2021).
30. Brombach, J.; Schröter, T.; Luecken, A.; Schulz, D. Optimizing the weight of an aircraft power supply system through a +/−270 VDC main voltage. *Gen* **2012**, *360*, 800.
31. Guedes, R.M. *Creep and Fatigue in Polymer Matrix Composites*, 2nd ed.; Woodhead Publishing Co., Ltd.: Duford, UK, 2019.
32. Bunge, C.A.; Gries, T.; Beckers, M. *Polymer Optical Fibers*; Woodhead Publishing Co., Ltd.: Duford, UK, 2017.
33. Tang, H.; Zhang, D.; Guo, S.; Qu, H. A Novel Model to Simulate Flexural Complements in Comliants Sensor Systems. *Sensors* **2018**, *18*, 1029. [CrossRef] [PubMed]
34. Lo, Y.; Chen, T.C.; Ho, T.L. Design in triangle-profiles and T-profiles of a wirebond using a linkage-spring model. *IEEE Trans. Compon. Packaging Manuf. Technol.* **2001**, *24*, 457–467.